Journal of Pathology
J Pathol 2022
Published online 4 January 2022 in Wiley Online Library (wileyonlinelibrary.com) DOI: 10.1002/path.5843

ORIGINAL ARTICLE

Estradiol promotes cell survival and induces *Greb1* expression in granulosa cell tumors of the ovary through an ERα–dependent mechanism

Victoria Cluzet[1], Marie M Devillers[1], Florence Petit[1], Alice Pierre[1], Frank Giton[2], Eloïse Airaud[1], David L'Hôte[1], Alexandra Leary[3], Catherine Genestie[4], Isabelle Treilleux[5], Anne Mayeur[6], John A Katzenellenbogen[7], Sung Hoon Kim[7], Joëlle Cohen-Tannoudji[1], Stéphanie Chauvin[1] and Céline J Guigon[1]*

[1] *Université de Paris, BFA, UMR 8251, CNRS, ERL U1133, Inserm, Paris, France*
[2] *AP-HP, Pôle Biologie-Pathologie Henri Mondor, INSERM IMRB U955, Créteil, France*
[3] *Gustave Roussy Cancer Campus and University of Paris-Saclay, Villejuif, France*
[4] *Department of Pathology, University Paris-Saclay, Gustave Roussy Cancer Center, Villejuif, France*
[5] *Department of Medical Oncology, Centre Léon-Bérard, Lyon, France*
[6] *Service de Médecine de la Reproduction et Préservation de la Fertilité, Hôpital Antoine Béclère, Clamart, France*
[7] *Department of Chemistry and Cancer Center at Illinois, University of Illinois at Urbana-Champaign, Champaign, IL, USA*

*Correspondence to: CJ Guigon, Université de Paris, 4 Rue MA Lagroua Weill-Hallé, 75201 Paris Cedex 13, France.
E-mail: celine.guigon@univ-paris-diderot.fr

No conflicts of interest were declared.

Abstract

Granulosa cell tumor (GCT) is a form of ovarian tumor characterized by its tendency to recur years after surgical ablation. Little is known about the mechanisms involved in GCT development and progression. GCTs can produce estradiol (E2), but whether this hormone could play a role in this cancer through its nuclear receptors, i.e. ERα and ERβ, remains unknown. Here, we addressed this issue by cell-based and molecular studies on human GCTs and GCT cell lines. Importantly, we observed that E2 significantly increased the growth of GCT cells by promoting cell survival. The use of selective agonists of each type of receptor, together with *Esr1* (ERα) or *Esr2* (ERβ)-deleted GCT cells, revealed that E2 mediated its effects through ERα-dependent genomic mechanisms and ERβ/ERα-dependent extra-nuclear mechanisms. Notably, the expression of *Greb1*, a prototypical ER target gene, was dose-dependently upregulated by E2 specifically through ERα in GCT cells. Accordingly, using GCTs from patients, we found that *GREB1* mRNA abundance was positively correlated to intra-tumoral E2 concentrations. Tissue microarray analyses showed that there were various combinations of ER expression in primary and recurrent GCTs, and that ERα expression persisted only in combination with ERβ in ∼40% of recurrent tumors. Altogether, this study demonstrates that E2 can promote the progression of GCTs, with a clear dependence on ERα. In addition to demonstrating that GCTs can be classified as a hormone-related cancer, our results also highlight that the nature of ER forms present in recurrent GCTs could underlie the variable efficiency of endocrine therapies.

Keywords: ovarian cancer; estradiol; estrogen receptor; GPER; GREB1; granulosa cell tumor; FOXL2

Received 27 May 2021; Revised 10 November 2021; Accepted 30 November 2021

No conflicts of interest were declared.

Introduction

Granulosa cell tumors (GCTs) represent about 5% of ovarian tumors and can affect women of all ages [1,2]. GCTs display two distinct clinical presentations: the juvenile form that is found predominantly in childhood and adolescence, and the adult form that occurs mainly in peri/post-menopausal women. Although this type of tumor is frequently diagnosed at an early stage of progression, it displays a high risk of late recurrence with metastases spread to the peritoneal cavity and liver [3]. Overall, chemotherapy and radiotherapy give unsatisfactory outcomes, as about 80% of patients with advanced tumors eventually die [4].

Patients with GCTs often display elevated circulating levels of inhibin B, anti-Müllerian hormone (AMH), and 17β-estradiol (hereafter referred as to E2) [1,5,6]. This hyperestrogenism leads to irregular menstruation, menorrhagia, inter-menstrual bleeding, and, in some cases, endometrial hyperplasia and adenocarcinoma [2]. Because of the known pro-carcinogenic action of E2 in several cancers and the reported expression of the

estrogen receptors α (ERα) and β (ERβ) in GCTs [7–9], it is assumed that E2 could promote the growth of primary and recurrent GCTs. Nevertheless, it has not been possible to verify this hypothesis experimentally because of the lack of cellular models with active ER signaling. Indeed, the available human GCT cell lines currently used, i.e. the metastatic KGN cells and the primary tumor COV434 cells, are unable to transactivate an estrogen-responsive reporter construct in response to E2 treatment, even upon overexpression of ERα and ERβ [10]. Besides, COV434 cells have been recently questioned as being of GCT origin, as they would eventually arise from a small cell carcinoma of the ovary [11]. Still, there are some arguments supporting the idea that E2 could play a role in this disease. Indeed, E2 increases the cell viability of GCT cells in primary cultures, at least from some adult GCTs [12]. In addition, hormonal therapies with aromatase inhibitors (AIs; anastrozole and letrozole) to decrease E2 synthesis can yield positive outcomes in patients with advanced or recurrent GCTs [13]. However, the effects of AIs are variable among patients, since some of them show little or no response [14]. This resistance may be attributable to the lack of ERs and/or of E2 in the patients, but screening of ER expression and determination of circulating E2 levels are not frequently performed prior to AI therapy. In addition, it is also possible that variable therapy responses are due to the type of ERs expressed in recurrent/metastatic GCTs. Indeed, ERα and ERβ could mediate opposite actions, as in most cancers ERα is generally reported to promote cell proliferation and survival, while ERβ would oppose these activities [15]. On the other hand, the role of ERβ in GCTs may be different from that described in most cancers, since this receptor, which is abundantly expressed in granulosa cells, is proposed to stimulate the growth and maturation of granulosa cells during folliculogenesis [16]. Besides, an additional level of complexity of E2 action resides in the fact that a third receptor, the G protein-coupled seven-transmembrane domain receptor GPER (G protein-coupled estrogen receptor), is expressed in about 90% of human GCTs [17]. Our previous cell-based studies using human GCT cell lines have suggested that E2 could exert an inhibitory action on the migration and invasion capacity through this atypical receptor [17].

In the present study, we sought to decipher the possible roles and mechanisms of action of E2 by performing cell-based and molecular analyses with a GCT cell line and human GCTs. Importantly, we demonstrate for the first time that E2 increased the growth of GCT cells by promoting their survival through ERα and ERβ, and not through GPER. ERα-mediated action could occur through a genomic pathway to stimulate the expression of *GREB1* (growth regulation by estrogen in breast cancer 1), an early-response gene that is a key regulator of E2-stimulated breast and epithelial ovarian cancer cell growth [18–21]. In contrast, ERβ signaling may occur via an extra-nuclear mechanism requiring ERα. Finally, our tissue microarray analyses revealed that primary and recurrent GCTs displayed GPER expression in most cases but exhibit strong variations in the levels and combination of ERα and ERβ. Overall, we demonstrate for the first time that GCTs can be definitively classified as a hormone-related cancer, and we propose that variable responses to AIs are possibly related to the strong differences in expression of estrogen receptors.

Materials and methods

Ethics approval and patient consent to participate

All women were fully counseled, and informed consent was obtained in writing from all participants. This investigation received the approval of the Internal Institutional Review Boards from Antoine Béclère Hospital (granulosa cells) and Institut Gustave Roussy (GCT). The study was performed in accordance with the Declaration of Helsinki.

Tissue microarrays of human granulosa cell tumors

Adult human GCTs were independently reviewed by two pathologists and collected by the National Rare Ovarian Tumor Observatory (TMRO) created by the National Investigators for Ovarian Cancer Studies (GINECO) group (France), as described previously [17]. We used 33 primary and 13 recurrent GCTs (supplementary material, Table S1). The search for the C402G *FOXL2* mutation in 28 and 9 of them, respectively, revealed that 93% of tested primary GCTs and 82% of tested recurrent GCTs display this mutation. Immunohistochemistry using specific ERα and ERβ antibodies [IR08461-2 (Agilent Technologies France, Les Ulis, France) and ab133467 (Abcam, Paris, France), respectively] was performed using the BenchMark ULTRA system (Roche Diagnostics, Meylan, France) with the UltraView Universal DAB Detection Kit (Roche Diagnostics). Because of the critical issue raised by the specificity of anti-ERβ antibodies [22], we confirmed the validity of the primary antibody against ERβ on human ovaries used as positive controls (supplementary material, Figure S1). This antibody recognizes the carboxy-terminal region of ERβ1. The expression of ERα and ERβ was assessed following two criteria: staining intensity (0: no staining; 1: weak; 2: intermediate; 3: strong) and percentage of stained cells. The immunoreactivity score was obtained by multiplying staining intensity by the percentage of stained cells.

AT29, KGN, MCF-7 cell lines and treatments

The AT29 cell line was provided by Dr N DiClemente (Centre de Recherche Saint-Antoine – UMR-S 938, Paris, France). This granulosa tumor cell line, which derives from GCTs of AT83 transgenic mouse, retains specific features of granulosa cells, such as steroidogenic factor 1 (SF-1), Wilms' tumor suppressor (WT-1), and anti-Müllerian hormone receptor 2 (AMHR2) expression [23]. The KGN cell line is a

metastatic granulosa cell line established from an adult patient with recurrent, metastasized GCT in the pelvic region [24]. It harbors the *FOXL2* C402G mutation described in most adult GCTs. It was purchased in 2011 from the RIKEN BioResource Center (RBRC-RCB1154, RIKEN Cell Bank, Ibaraki, Japan) after approval by Dr Yoshiro Nishi and Dr Toshihiko Yanase. GCT cell lines were cultured at 37 °C with 5% CO_2 in Dulbecco's modified Eagle's medium (DMEM)/F12 (Gibco, Thermo Fisher Scientific, Illkirch-Graffenstaden, France), with phenol red (PR), containing 10% fetal bovine serum (FBS) and 0.5% penicillin/streptomycin (PS). MCF-7 cells were purchased from ATCC (LGC Standards SARL, Molsheim, France) and cultured at 37 °C with 5% CO_2 in DMEM (Gibco), with PR, containing 10% FBS and 0.5% PS. For all assays except MTT, caspase-3/7 activity, and BrdU incorporation assays (see below), cells were seeded in cell culture plates with PR-free DMEM/F12 (Gibco), containing 10% charcoal-dextran-stripped fetal bovine serum (CD-FBS) and 0.5% PS for 24 h. Cells were then cultured with PR-free DMEM/F12 medium without FBS (FBS and PR-free medium) for 24 h prior to their treatment with either 17β-estradiol [0.1, 1 or 10 nM, Tocris (Bio-Techne SAS, Noyal Châtillon-sur-Seiche, France)], PPT (10 nM, Tocris), DPN (10 nM, Tocris), or G-1 (50 nM, Tocris), or their respective vehicles [0.1% ethanol and/or 0.1% dimethyl sulfoxide (DMSO)] for the indicated times. Only cell batches below 40 passages were used.

Esr1 and *Esr2* deletion by CRISPR/Cas9 in AT29 cells

Esr1 and *Esr2* deletion by CRISPR/Cas9 was performed by the TACGENE core facility (Museum National d'Histoire Naturelle, Paris, France). Single guide RNA (sgRNA) sequences were chosen in the third and second exons of the *Esr1* and *Esr2* genes (after the ATG codon), respectively, with the CRISPOR tool (http://crispor.org) based on specificity and efficiency scores and cloned into the plasmid PX458. AT29 cells were transfected with AMAXA nucleofection (Kit V, Program V-005; Lonza, Levallois-Perret, France). Seventy-two hours after transfection, GFP-positive cells were sorted by FACS and isolated in a 96-well plate. To obtain $Esr1^{-/-}$ clones, cells were co-transfected with pX458 plasmids expressing sgRNA-1 (GTGCAGCAAGGCCATTCCC G) and sgRNA-2 (TCCCGAGGCTTTGGTGTGAA). Ten clones were screened by PCR and Sanger sequencing of the targeted region of *Esr1* gene, using the Synthego online tool (https://www.synthego.com/products/bioinformatics/crispr-design-tool). Three clones, named #A1, #B1, and #C1, with a homozygous mutant sequence exhibiting genomic deletions were confirmed to lack *Esr1* protein expression by western blotting (supplementary material, Figure S2A) with a primary antibody against ERα (#04-820; Sigma-Aldrich Chimie SARL, Saint-Quentin Fallavier, France) following a protocol described previously [17]. For the $Esr2^{-/-}$ clones, we used the following sgRNAs: sgRNA-3 (GCTTTACCTGTTTACAGGCA) and sgRNA-4 (AGTGATCTTGCTTCACACCA), leading to an excision of 31 base pairs (bp); and sgRNA-4 (AGTGATCTTGCTTCACACCA) and sgRNA-5 (AGAGAAGCGATGATTGGCAG), resulting in a 43-bp deletion (supplementary material, Figure S2B). Forty-seven clones were screened by PCR and Sanger sequencing of the targeted region of the *Esr2* gene. Two clones (#D2 and #G22) with a genomic deletion on the *Esr2* sequence were selected for further analysis. To confirm these deletions, RNA was extracted, reverse-transcribed as described below, and cDNAs were amplified by PCR with primers encompassing the deletions: *mEsr2-F1*: TGTAGAGAGCCGTCACGAAT; *mEsr2-R1*: CACAGGACCAGACACCGTAA. Purified PCR products were then sequenced to check for the deletions (Eurofins Genomics, Ebersberg, Germany). The predicted protein sequence was deduced based on these deletions (supplementary material, Figure S2B).

Transient transfection of AT29 and MCF-7 cells, and Dual® luciferase reporter assays

The firefly luciferase reporter construct containing three EREs (3xERE-TATA-LUC; Addgene LGC Standards, Teddington, UK) or six copies of an AP-1-response element (AP-1 pGL4.44 LUC2P/AP1 RE/Hygro; Promega, Charbonnières-les-Bains, France) was used in this study. The control plasmid pRL-TK, carrying the *Renilla* luciferase gene under the control of the *TK* promoter (Promega), was co-transfected to correct for variations in transfection efficiency. For transient transfection assays, AT29 and MCF-7 cells were seeded in 96-well plates at 1.7×10^4 cells per well in 10% CD-FBS PR-free DMEM/F12 medium for 24 h. The reporter (ERE- or AP-1 sequences, pGL2 or pGL4.44 backbones at 125 ng/well) and the control (*Renilla* at 20 ng/well) plasmids were transfected for 6 h using Lipofectamine 2000 reagent (Thermo Fisher Scientific) in Opti-MEM medium (Thermo Fisher Scientific) according to the manufacturer's protocol. Then the medium was replaced with a 10% CD-FBS PR-free DMEM/F12 medium. After 24 h, cells were treated with vehicle or different drugs for another 24 h. At the end of the experiment, cultures were lysed in Passive Lysis Buffer (Promega). Luciferase activities were determined using the Dual Luciferase Reporter Assays System (Promega) and the Berthold Lumat LB9507 luminometer (Berthold France, Thoiry, France). The transactivation activity resulting from firefly luciferase was normalized to that of *Renilla* luciferase.

Granulosa cells and granulosa cell tumors from patients

Granulosa cells were obtained from patients undergoing *in vitro* fertilization at Antoine Béclère Hospital (France). All women met the following inclusion criteria: (1) age between 20 and 40 years old; (2) both ovaries present, with no morphological abnormalities, and

Table 1. Clinical information of the patients.

Sample	Tumor stage	Patient age (years)	No. of relapses from initial diagnosis	Sample pre- or post-chemotherapy	Survival after sampling	*FOXL2* C402G mutation status
1	Recurrent	53	One relapse after 10 years	Post	Dead	Heterozygous
2	IA	49	Initial diagnosis	Pre	Alive 9 years post-sample	Heterozygous
3	Recurrent	50	Four relapses within 17 years	Pre	Alive 10 years post-sample	Heterozygous
4	Recurrent	50	Three relapses within 10 years	Pre	Alive 10 years post-sample	Heterozygous
5	Recurrent	54	Two relapses within 11 years	Pre	Alive 6 years post-sample	Homozygous
6	Recurrent	67	One relapse after 9 years	Pre	Dead	Heterozygous

adequately visualized in transvaginal ultrasound scans; (3) menstrual cycle length range between 26 and 30 days; (4) no current or past diseases affecting the ovaries or gonadotropin and sex steroid secretion, clearance, or excretion; (5) no clinical signs of hyperandrogenism; and (6) no polycystic ovary morphology at ultrasonography. Infertility was due either to tubal or to sperm abnormalities. All women were fully counseled, and informed consent was obtained in writing from all participants. This investigation received the approval of the Institutional Review Board from Antoine Béclère Hospital. After oocyte isolation, follicular fluids (FF) were pooled. Granulosa cells were then purified as previously described [25]. Briefly, FF was centrifuged through a one-step density Percoll gradient [vol/vol, Dulbecco's phosphate-buffered saline (DPBS)/Percoll] at 4000 × *g* for 15 min to remove red blood cells. Granulosa cells were collected at the interface, washed with DPBS, and stored at −80 °C until use. We used six adult GCTs (one GCT at the IA stage and five recurrent GCTs) expressing both ERα and ERβ, previously reviewed by a pathologist at the Institut Gustave Roussy (Villejuif, France) and stored at −80 °C (Table 1). We analyzed samples displaying at least 80% of tumor granulosa cells, as determined on hematoxylin and eosin-stained histological slides. We characterized the presence of the C402G *FOXL2* mutation by sequencing GCT cDNA products obtained after reverse transcription, as described below, amplified by PCR with the Platinum SuperFi II DNA Polymerase (Invitrogen) using the following primers: *hFOXL2-F*: 5′-CACAACCTCAACGAGTGC-3′, *hFOXL2-R*: 5′-TTGC CGGGCTGGAAGTGCG-3′, yielding a 182 bp product, as described previously [26].

RNA extraction, reverse transcription, and qPCR

AT29 and KGN cells were seeded at a density of 1×10^5 cells/ml in 12-well plates in 10% CD-FBS PR-free medium and treated with the indicated drugs for 6 or 24 h. They were lysed in RLT buffer from the RNeasy Mini Kit (# 74106; Qiagen, Courtaboeuf, France) and RNAs were extracted following the manufacturer's protocol. Total RNAs from human GCTs were obtained using the RNeasy Mini Kit following the procedure described previously [27]. Total RNAs from purified human granulosa cells were extracted using TRIzol reagent according to the manufacturer's protocol. The extraction quality control and concentration of RNAs were performed as described previously [17]. Total RNAs (1 µg) were reverse-transcribed using Invitrogen Superscript II (Thermo Fisher Scientific) and random primers (9 ng/ml final) (Promega) following the manufacturer's instructions. Primers used for quantitative real-time PCR were designed using Primer-BLAST (National Institutes of Health) and obtained from Eurofins (supplementary material, Table S2). Real-time qPCR was performed using a Lightcycler® 480 SYBR Green I Master and Lightcycler® 480 instrument (Roche Molecular Biochemicals, La Rochelle, France), as described previously [27]. All samples were run in triplicates. For each primer pair, a standard curve was generated using serial dilutions of cDNA (1/10, 1/20, 1/50, and 1/100) prepared from AT29 or KGN cell cDNAs or a mix of granulosa cells and GCT cDNAs to determine the efficiency of amplification. Melt-curve analysis and electrophoresis of amplified products confirmed that only a single product of the expected size was generated. Quantification of target gene expression was normalized to that of a reference gene, i.e. β2-microglobulin (mouse *B2m*), hypoxanthine phosphoribosyltransferase 1 (mouse *Hprt* and human *HPRT*) or D-glyceraldehyde-3-phosphate dehydrogenase (human *GAPDH*), depending on the experiment, and expressed as relative levels.

AT29 cell growth assay

MTT [3-(4,5-dimethylthiazol-2-yl)-2,5-diphenyl tetrazolium bromide, Sigma] assays were conducted as described previously [17]. AT29 cells were seeded at a density of 1×10^4 cells/ml in 24-well plates in 10% CD-FBS PR-free DMEM/F12 medium. Twenty-four hours later, cells received the indicated treatments in FBS and PR-free medium. At each treatment time studied (0, 24, 48, and 72 h), cells were incubated with MTT (5 mg/ml in DPBS; Gibco) for 2 h at 37 °C and then lysed in DMSO. The optical density (OD) of cellular lysates was measured at 575 nm using a FlexStation 3 (Molecular Devices, San José, CA, USA).

AT29 cell apoptosis by caspase-3/7 activity assay

Cell apoptosis was evaluated using the Caspase-Glo®3/7 Assay System (# G8091; Promega) in line with the manufacturer's instructions. Cells were seeded at a density of 2.4×10^5 cells/ml (100 µl per well) in 96-well plates, with white walls and a clear bottom, in 10% CD-FBS PR-free DMEM/F12 medium. Twenty-four hours later, cells received the indicated treatments for 24 h in FBS

and PR-free medium. Then 100 µl of Caspase-Glo reagent was added to each well and the kinetics of luminescence intensity was measured using a microplate reader (Flexstation 3; Molecular Devices) for 4 h at room temperature. For each sample, the maximal caspase-3/7 activity obtained during kinetics was normalized to that of the vehicle control.

AT29 cell proliferation by BrdU incorporation assay

Cells were seeded at a density of 2×10^4 cells/ml in eight-well culture slides (Falcon #354118, Sigma-Aldrich) in 10% CD-FBS PR-free DMEM/F12 medium and treated 24 h later with the indicated drugs in FBS and PR-free medium for 24 h. At the end of the treatments, AT29 cells were incubated for 2 h at 37 °C with BrdU at 10 µM in FBS and PR-free medium. Cells were washed twice with PBS 1X (Euromedex, Soufferweyersheim, France) and then fixed with 4% paraformaldehyde (PFA) for 15 min at room temperature. After three PBS washes, cells were permeabilized with 0.1% Triton in PBS with 1% bovine serum albumin (BSA) for 6 min and with 2 N HCl for 20 min. Cells were washed three more times with PBS, incubated for 1 h with PBS–3% BSA (blocking buffer) at room temperature, and then incubated overnight at 4 °C with a rabbit anti-BrdU antibody (ab152095; Abcam) (1:200) diluted in blocking buffer. The next day, cells were washed three times with 0.1% Tween-20 in PBS and incubated for 1 h at room temperature with a goat Alexa Fluor®488 anti-rabbit antibody (A11070, 1:2000; Thermo Fisher Scientific) diluted in the blocking buffer. After washes with 0.1% Tween-20 in PBS, coverslips were mounted on glass slides with a mounting medium containing 4,6-diamidino-2-phenylindole (DAPI; Sigma). BrdU-positive proliferating cells and DAPI-positive cells were counted from four different field photographs at a 10× magnification obtained after laser excitation for DAPI (405 nm) and FITC (488 nm) using a fluorescence microscope (Nikon Eclipse 90i). Cell counting was performed using ImageJ software (ImageJ 1.47t; Wayne Rasband, National Institutes of Health, Bethesda, MD, USA). The labelling index was established by calculating the ratio of the number of BrdU-positive cells to the total number of DAPI-positive cells in each field, with a minimum of 100 cells counted per well.

Cell migration and invasion assays

Cells were serum-starved for 24 h before the experiment with FBS and PR-free DMEM/F12 medium. Transwell inserts (Corning SAS, Boulogne-Billancourt, France) were rehydrated with FBS and PR-free medium, and then left at 37 °C for 24 h. For invasion assays, inserts were coated with Matrigel matrix (100 µg/ml; BD Biosciences, San José, CA, USA) diluted in FBS and PR-free medium. On the day of the experiment, bottom wells were filled with 10% CD-FBS PR-free DMEM/F12 medium. AT29 cells were harvested by gentle trypsinization and seeded at a density of 5×10^4 cells per Transwell in FBS and PR-free medium in the presence of the indicated drugs (time 0). After 4.5 h at 37 °C, cells were fixed in 4% PFA for 40 min at room temperature and then rinsed in PBS. Cells located on the inner side of the Transwell (non-migrating cells) were removed with a cotton swab. Membranes from Transwells were mounted on glass slides with a mounting medium containing DAPI to observe the migrated cells located on the outer side of the Transwell using a fluorescence microscope. For each Transwell, five different fields were photographed at 10× magnification. Cell counting was performed using ImageJ software. Relative numbers of migrated or invading cells were calculated by normalizing to the number of migrated or invading cells in the control condition.

Estradiol level measurements

The amount of E2 present in human granulosa cells and in GCTs was determined by mass spectrometry coupled with gas chromatography (GC–MS) procedure and normalized to the quantity of proteins in the sample, as described previously [28].

Statistical analyses

Data were analyzed using Prism 6 (version 6.0; GraphPad Software, San Diego, CA, USA). We used non-parametric tests when samples were not normally distributed as determined by Shapiro–Wilk normality tests. Depending on the experimental setting, we used unpaired Student's *t*-tests (Mann–Whitney), parametric and non-parametric one-way ANOVA (Kruskal–Wallis), paired non-parametric one-way ANOVA (Friedman test), two-way ANOVA, chi-squared tests, and linear regression. Data are shown as means ± SD or in scatter plots with means. $p < 0.05$ was considered as statistically significant.

Results

ERα and ERβ expression varies in adult GCTs

We examined ERα and ERβ protein expression in the same tissue microarrays (TMAs) of 33 primary and 13 recurrent GCTs as those used for analyzing GPER expression [17] with validated antibodies (Figure 1A and supplementary material, Figure S1). We could detect ERα or ERβ in 70–80% of primary and recurrent GCTs, with wide heterogeneity in their immunoreactivity score (Figure 1B). This was due to large variations in the cell staining intensity and in the percentage of positive cells, as 10–80% of cells expressed ERα or ERβ (Figure 1C). Analysis of ER subcellular localization indicated that ERα was primarily localized in the nucleus of tumoral granulosa cells in all studied samples. In contrast, ERβ could be observed in both nuclear and cytoplasmic compartments, as depicted in a prior study [8].

When we analyzed the data collected on both ERα and ERβ immunostaining for each tumor, we observed that

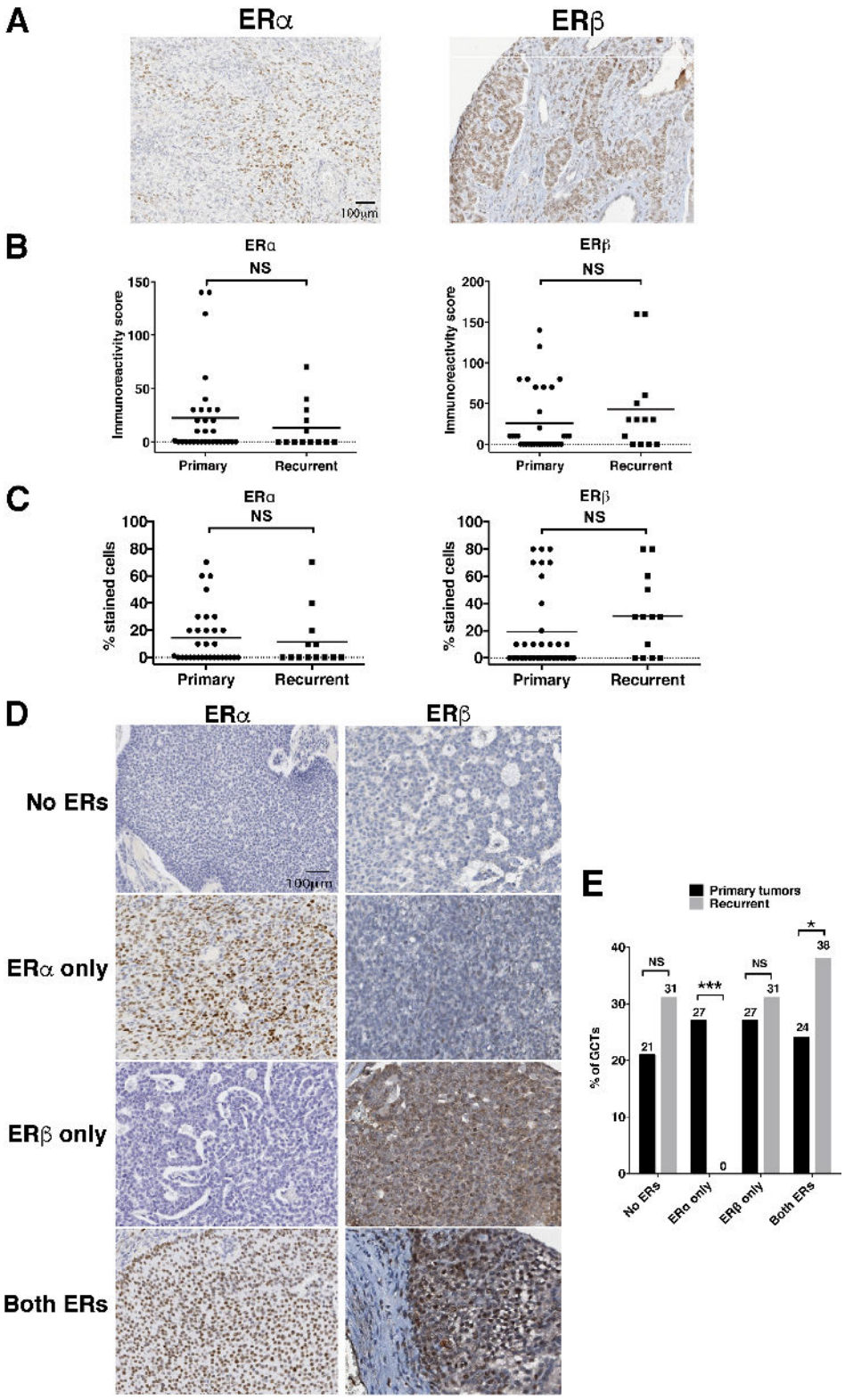

Figure 1. Different combinations of ERα and ERβ expression exist in primary and recurrent GCTs. (A) Immunodetection of ERα and ERβ in the primary tumor of one patient, displaying 20% of ERα-positive cells (staining intensity: 1) and 80% of ERβ-positive cells (staining intensity: 2). Scale bars: 100 µm. (B, C) Immunoreactivity score and percentage of stained cells for ERα and ERβ in 33 primary and 13 recurrent tumors on tissue microarrays (TMAs). Each dot corresponds to one tissue sample and bars represent the means. Data were analyzed using a non-parametric *t*-test (Mann–Whitney). NS, not significant. (D) Immunodetection of ERα and ERβ on TMAs of adult GCTs. Pictures of the four different ER combinations existing in GCTs are shown. In the first row, a recurrent GCT with no ERα and no ERβ expression (no ERs) is shown. In the second row, this primary GCT exhibits ERα expression essentially in the nucleus, while ERβ is absent (ERα only). In the third row, this primary GCT displays ERβ staining in both the nucleus and the cytoplasm, while no ERα expression is detected (ERβ only). In the fourth row, this recurrent GCT displays both ERα and ERβ expression (both ERs). ERα shows a preferential localization in the nucleus, while ERβ is present in the nucleus and in the cytoplasmic compartments. Scale bars: 100 µm. (E) Percentage of GCTs exhibiting each combination of ERs in the 33 primary and 13 recurrent GCTs. Data were analyzed using chi-squared tests. NS, not significant; $^{*}p < 0.05$, $^{***}p < 0.001$.

the levels of these two receptor subtypes varied greatly between GCTs (Figure 1D). Indeed, there was a notable fraction of primary GCTs lacking ER expression (21%), others expressing either ERα or ERβ (27% of each), and others exhibiting both receptors (24%) (Figure 1E). ER levels dramatically changed during tumor progression, since compared with primary GCTs, there was a significant increase in the percentage of recurrent GCTs expressing both ERα and ERβ (24% versus 38%, $p < 0.05$, Figure 1D,E). Besides, recurrent GCTs did not exhibit expression of ERα alone, in contrast to primary GCTs (0% versus 27%, $p < 0.001$, Figure 1E). Examination of the GCTs not expressing ERs revealed that they nonetheless expressed GPER (supplementary material, Figure S3). Overall, these data reveal the strong variability in the nature of estrogen receptors present in GCTs, with ERα being found only in combination with ERβ at advanced stages.

E2 increases growth of tumor granulosa cells by promoting their survival through ERα and ERβ

To evaluate the effects of E2 on different cellular processes underlying tumorigenesis, i.e. survival, proliferation, migration, and invasion, we used the AT29 cell line, which was obtained from a large primary tumor of a transgenic mouse model of GCTs exhibiting similar endocrine, cellular, and molecular alterations to those observed in humans [23,27,29]. Our RT-qPCR analyses showed that this cell line shares molecular characteristics with human GCTs, and to some extent with KGN cells. Indeed, AT29 cells express inhibin α (*Inha*), βA (*Inhba*), and βB (*Inhbb*) subunit genes (supplementary material, Figure S4). In addition, they also displayed expression of *STAR* and *AMH* but not that of *CYP19A1* [12,29,30] (supplementary material, Figure S4). *FSHR* transcripts were not detected, as in about 10% of human GCTs [12]. AT29 cells retained *Foxl2* expression (supplementary material, Figure S4), and DNA sequencing analysis revealed that *Foxl2* did not display the C402G mutation observed in adult human GCTs [26] (data not shown).

As E2 can mediate its actions through ERα, ERβ, and GPER, we analyzed their potential contribution by treating AT29 cells with their selective agonists, i.e. PPT for ERα, DPN for ERβ, and G-1 for GPER, at classically used concentrations [31–33]. By measuring cell growth using MTT assays, we observed that E2 significantly increased the size of the cell population after 72 h of treatment (Figure 2A). PPT and DPN both mimicked this effect of E2, whereas G-1 did not (Figure 2A). As cell growth can result from alterations in cell survival and/or proliferation, we further evaluated which of these processes were altered by E2 in these cells. Notably, E2 treatment led to a modest but significant decrease in caspase-3/7 activity by about 10% after only 24 h, compared with the control condition (Figure 2B). Either PPT or DPN decreased caspase-3/7 activity, while G-1 had no effect (Figure 2B). In contrast, there was neither E2-induced nor PPT or DPN change in BrdU incorporation in comparison with that in the control condition (Figure 2C). E2, as the ERα and ERβ agonists, did not alter cell migration or invasion capacities (Figure 2Da,b). In contrast, G-1 had a modest but significant inhibitory effect on these two processes (Figure 2Dc,d). These findings suggest that E2 could enhance the growth of AT29 cells by promoting their survival through ERα and ERβ, but not through GPER.

To further investigate the role of the ERs in granulosa tumor cell growth and survival, we then used the CRISPR/Cas9 genome editing system to generate AT29 cell clones harboring nucleotide deletions in the first coding exons of *Esr1* ($Esr1^{-/-}$, clones #A1, #B1) or *Esr2* ($Esr2^{-/-}$, clones #D2, #G22), leading to the truncation and loss of function of ERα or ERβ, respectively. In $Esr1^{-/-}$ clones, treatments with E2 for 72 h had no impact on cell growth compared with that of the wild-type (WT) clones, as revealed by MTT assays (Figure 3A). In line with these findings, there was no E2-induced alteration in caspase-3/7 activity in $Esr1^{-/-}$ cells, in contrast with WT cells, where E2 significantly decreased it (Figure 3B). As expected, there was no effect on cell proliferation in either WT or $Esr1^{-/-}$ cells, as shown by BrdU incorporation assays (Figure 3C and supplementary material, Figure S5). In $Esr2^{-/-}$ clones, E2 treatment for 72 h increased cell growth, similarly to that seen in WT cells (Figure 3A). Accordingly, E2 treatment significantly inhibited caspase-3/7 activity without affecting BrdU incorporation in both WT and $Esr2^{-/-}$ cells (Figure 3B,C and supplementary material, Figure S5).

DPN is reported to have a 70-fold higher relative binding for ERβ than for ERα (EC_{50} values are 0.85 and 66 nM, respectively) [32]. However, to ascertain that the observed stimulatory action of DPN on AT29 growth and survival did not result from the lack of specificity of this agonist, we next investigated its effect on the growth of $Esr2^{-/-}$cells lacking ERβ but still expressing ERα. We observed in those clones that this agonist totally lost its cell growth stimulatory effect (Figure 3D), thus confirming that DPN specifically acted through ERβ to mediate its action in AT29 cells. Overall, these findings indicate that E2 would promote cell growth and survival in GCT cells expressing either ERα or ERβ, on the condition that ERα is present.

ERα, but not ERβ, mediates its action through the genomic pathway in AT29 cells

We wanted to gain further insights into the possible molecular mechanisms whereby ERα and ERβ could exert their regulatory action in AT29 cells. E2 treatment of ERE-LUC-transfected AT29 cells upregulated luciferase activity by about four-fold, implying that ERs could act through the genomic pathway (Figure 4A). However, PPT induced an approximately three-fold increase of the ERE-LUC reporter activity, while DPN had no effect (Figure 4A). Co-treatment of these cells with DPN and PPT increased luciferase activity to the same extent as PPT treatment alone, suggesting that only

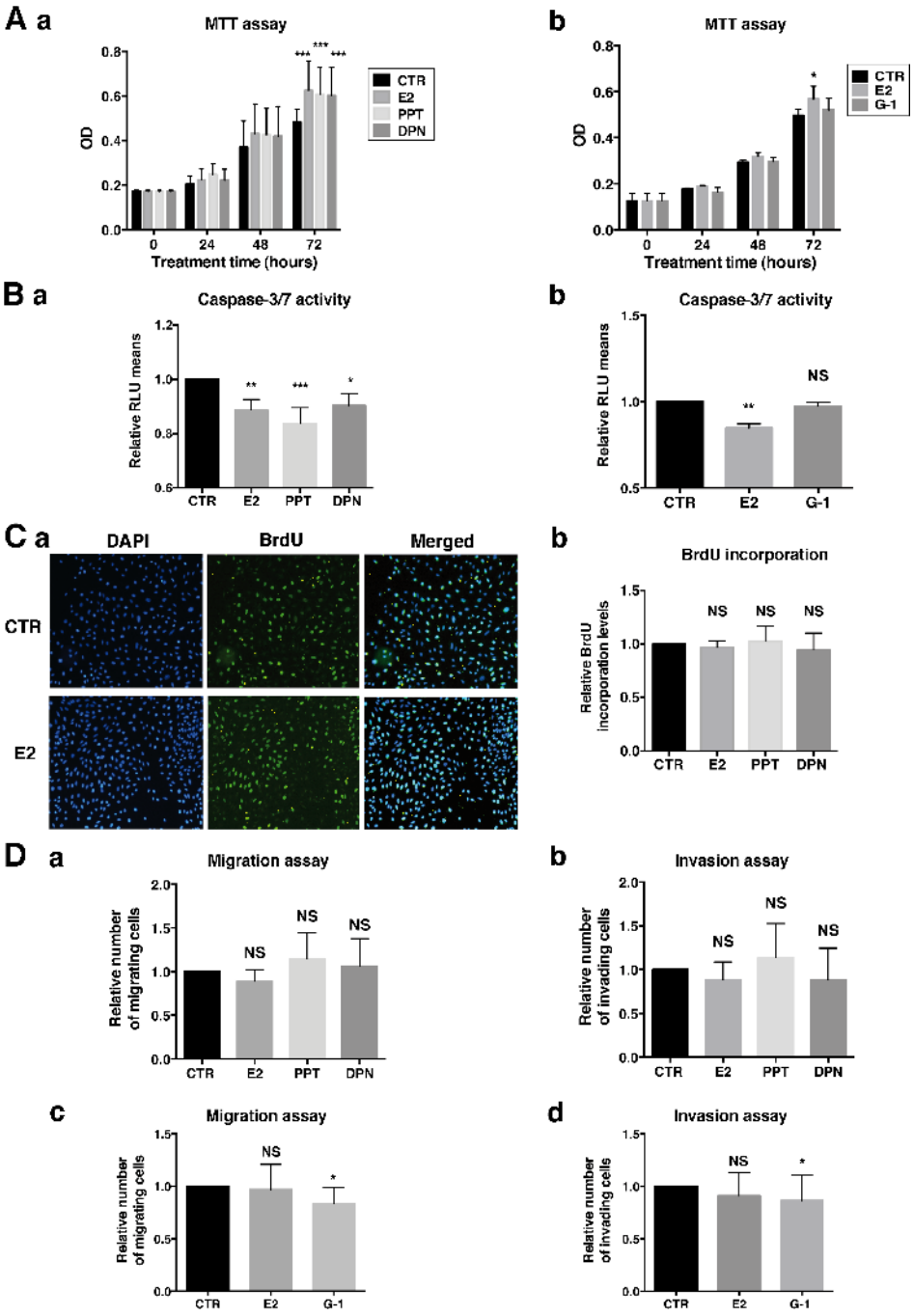

Figure 2. E2 and the selective agonist of either ERα or ERβ, but not that of GPER, promote AT29 cell growth and survival. (A) Cell numbers were assessed using MTT assays on AT29 cells treated for the indicated times (a) with control (CTR) vehicle, E2 (10 nM), PPT (10 nM) or DPN (10 nM), and (b) with control (CTR) vehicle, E2 (10 nM) or G-1 (50 nM). Optical density (OD) measurement correlates with cell number. Graphs show the results obtained from three or four independent experiments for each group. (B) Cell apoptosis was analyzed by measuring caspase-3/7 activity in AT29 cells treated with (a) control (CTR) vehicle, E2 (10 nM), PPT (10 nM) or DPN (10 nM) or (b) control (CTR) vehicle, E2 (10 nM) or G-1 (50 nM) for 24 h. Caspase-3/7 activity was assessed as relative luminescence unit (RLU) after normalization using the control condition. The number of experiments for each group was as follows: (a) CTR: 7, E2: 7, PPT: 5, and DPN: 7; (b) CTR: 5, E2: 4, and G-1: 3. (C) Labelling index (% cells incorporating BrdU) was determined by immunolabeling assays of AT29 cells treated with either control (CTR) vehicle, E2 (10 nM), PPT (10 nM) or DPN (10 nM) for 24 h. (a) Representative pictures of DAPI (blue) and BrdU incorporation (green) immunolabeling and merged images for CTR and E2 treatment condition are shown. (b) Relative BrdU incorporation was calculated by dividing the number of BrdU-positive cells by the total number of cells, as assessed by the number of DAPI-positive cells, and normalized to that of the control conditions. The results obtained from CTR: 7, E2: 7, PPT: 6, and DPN: 6 independent experiments are shown. (D) Migration and invasion capacity assays assessed using Transwell inserts for AT29 cells treated with (a, b) control (CTR) vehicle, E2 (10 nM), PPT (10 nM) or DPN (10 nM) and (c, d) control vehicle (CTR), E2 (10 nM) or G-1 (50 nM) for 4.5 h. The results of migration and invasion assays from at least three independent experiments are shown, with graphs representing the relative number of migrating or invading cells counted in a field normalized to the number of migrating or invading cells, respectively, of control (CTR) conditions. For each assay of this figure, the horizontal and error bars represent the means ± SD, respectively. Data in A were analyzed with a paired two-way ANOVA test; in B–Db with a non-parametric one-way ANOVA test (Kruskal–Wallis); and in Dc, d with a parametric one-way ANOVA test. $^{*}p < 0.05$, $^{**}p < 0.01$, $^{***}p < 0.001$; NS, not significant.

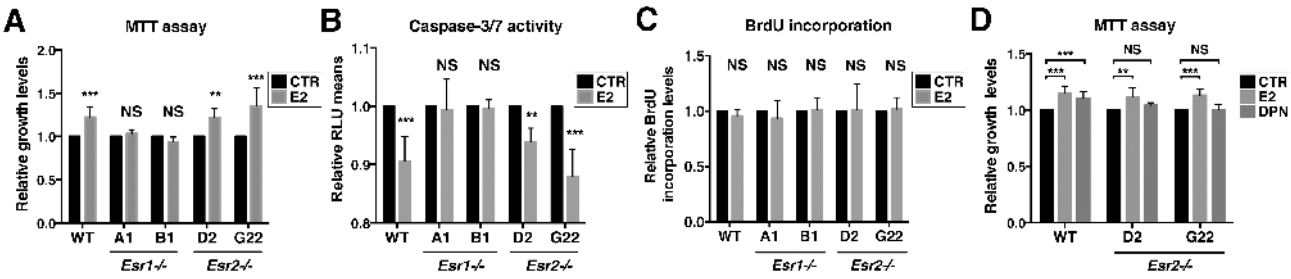

Figure 3. E2 requires ERα to promote AT29 cell growth and survival. (A) Cell numbers were assessed using MTT assays of wild-type (WT) and *Esr1*$^{-/-}$ AT29 cells or *Esr2*$^{-/-}$ AT29 cells treated for 72 h with either control (CTR) vehicle or E2 (10 nM). The graphs show the relative growth levels corresponding to OD values, normalized to that of the control conditions for each clone, collected from at least three independent experiments (WT clone: $n = 8$; clone #A1: $n = 5$; clone #B1, $n = 3$; clone #D2, $n = 3$; clone #G22, $n = 3$). (B) The apoptosis of AT29 cells was assessed by measuring caspase-3/7 activity in WT, *Esr1*$^{-/-}$, and *Esr2*$^{-/-}$ AT29 cells treated for 24 h with either control (CTR) vehicle or E2 (10 nM). Caspase-3/7 activity was assessed as relative luminescence units (RLU) after normalization to the control condition. The number of independent experiments for each group was as follows: WT clone, $n = 11$; clone #A1, $n = 6$; clone #B1, $n = 3$; clone #D2, $n = 4$; and clone #G22, $n = 4$. (C) Labelling index (% cells incorporating BrdU) was determined by immunolabeling assays of WT, *Esr1*$^{-/-}$ or *Esr2*$^{-/-}$ AT29 cells treated with either control (CTR) vehicle or E2 (10 nM) for 24 h. The relative BrdU incorporation level was normalized to that of the control condition. The number of independent experiments for each group was as follows: WT clone, $n = 6$; clone #A1, $n = 3$; clone #B1, $n = 3$; clone #D2, $n = 3$; and clone #G22, $n = 3$. (D) Determination of cell growth by MTT assays in WT or *Esr2*$^{-/-}$ cells treated for 72 h with either control (CTR) vehicle, E2 (10 nM) or DPN (10 nM). The graphs show the relative growth levels corresponding to OD values normalized to that of the control conditions for each clone. The number of experiments for each group was as follows: WT clone, 8; clone #D2: 4; and clone #G22: 4. The horizontal and error bars represent the means ± SD, respectively. Data were analyzed using paired two-way ANOVA tests. $^{*}p < 0.05$, $^{**}p < 0.01$, $^{***}p < 0.001$; NS, not significant.

ERα regulates gene transcription through the classical genomic pathway. We also tested whether ERs mediate their effects via non-ERE regulatory mechanisms by tethering to transcription factor complexes such as activator protein 1 (AP-1) [34]. However, E2 treatment did not modify the AP-1-dependent luciferase reporter gene activity in AT29 transfected cells (Figure 4B). Treatment with 8-Br-cAMP, which can drive AP-1-dependent gene expression [35], did not show any effect on AP-1-reporter gene activity (Figure 4B), whereas it stimulated by about three-fold the AP-1-dependent luciferase activity in MCF-7 transfected cells (supplementary material, Figure S6). Taken together, our findings suggest that ERα, but not ERβ, mediates E2 action on cell growth and survival through an ERE-dependent signaling pathway.

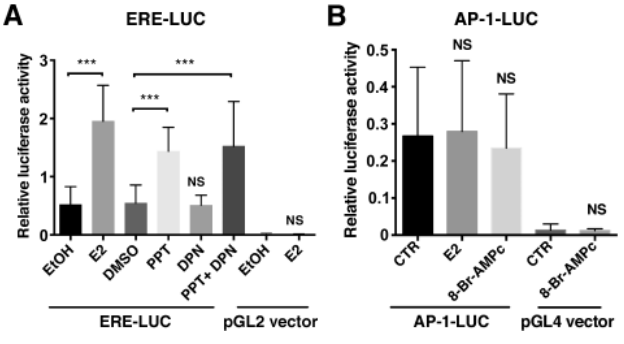

Figure 4. E2 could mediate its action via ERα, but not via ERβ, through classical genomic pathways in AT29 cells. (A) Relative luciferase activity of ERE-LUC vector or pGL2 vector (backbone) in AT29 cells treated for 24 h with E2 (10 nM), PPT (10 nM), DPN (10 nM) or related vehicles (ethanol and DMSO). The number of independent experiments was four. (B) Relative luciferase activity of AP-1-LUC vector or pGL4 vector (backbone) in AT29 cells treated for 24 h with E2 (10 nM) or 8-Br-cAMP (1 mM) or control vehicle (CTR). The graph shows the results obtained from four independent experiments with transfections performed in six replicates for each condition. The relative luciferase activity was determined by the activity of the firefly luciferase normalized to that of the *Renilla* luciferase in each sample. Data were analyzed with non-parametric one-way ANOVA (Kruskal–Wallis).

GREB1 abundance is regulated by E2 concentrations via ERα in GCTs

As we identified that E2-bound ERα can transactivate an ERE-luciferase reporter gene, we hypothesized that *Greb1*, a highly E2-upregulated gene in breast and epithelial ovarian cancers [18–21], may well be induced by E2 in GCTs. Indeed, in AT29 cells, E2 dramatically upregulated *Greb1* relative mRNA levels by about 4- to 5-fold and 11-fold after 6 and 24 h of treatment, respectively (Figure 5A). Treatment with the ERα agonist, PPT, fully reproduced the E2 stimulatory effect on *Greb1* abundance, as PPT treatment led to a 4- to 5-fold and a 10-fold induction at 6 and 24 h, respectively, whereas the ERβ agonist, DPN, had no effect (Figure 5A). Accordingly, *Greb1* induction observed after a 24 h E2 treatment was totally lost in *Esr1*$^{-/-}$ cell clones, but not in *Esr2*$^{-/-}$ clones (Figure 5B). Importantly, E2 dose-dependently stimulated *Greb1* expression in AT29 cells, with induction becoming significant at 1 nM (Figure 5C).

We measured *GREB1* transcript relative abundance and E2 content in both GCTs and control granulosa cells retrieved by an ovary stimulation protocol, to establish a possible regulation of *GREB1* levels by E2 concentrations *in vivo*. Both GCTs and granulosa cells expressed both ERα (*ESR1*) and ERβ (*ESR2*), as determined by RT-qPCR (Figure 5D and supplementary material, Figure S7). We observed that *GREB1* had a 2- to 3-fold lower relative expression level in GCTs than in

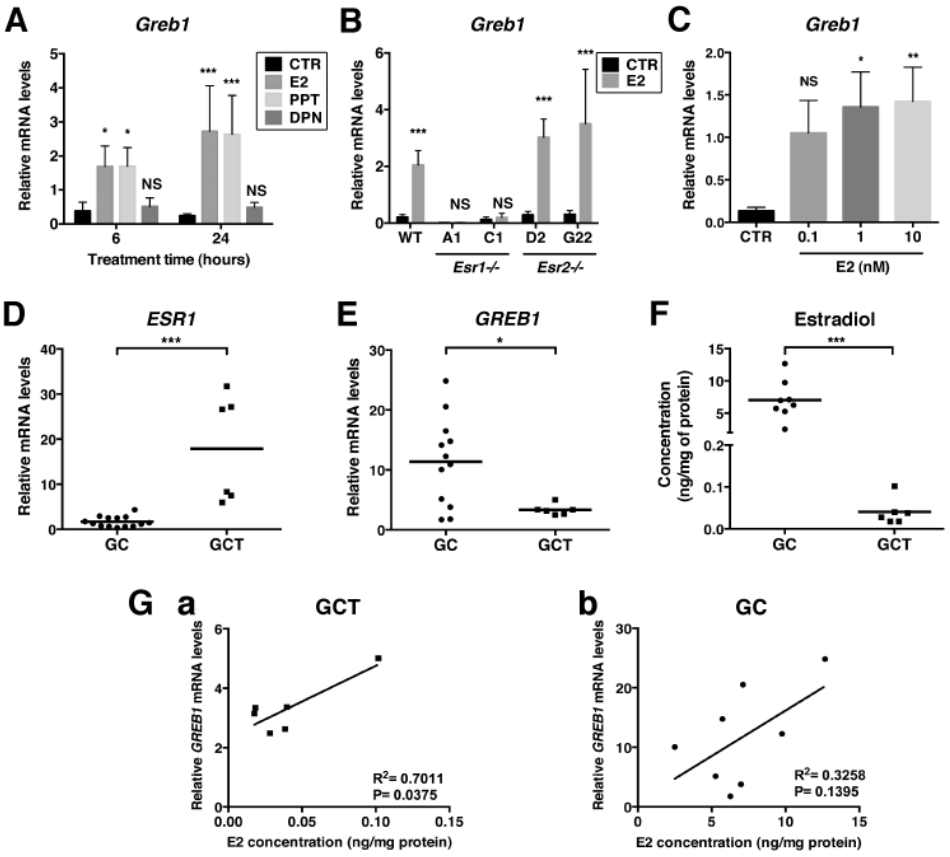

Figure 5. *GREB1* abundance could be regulated by E2 concentrations in GCTs. (A) Relative levels of *Greb1* mRNA in AT29 cells treated for the indicated times with either control vehicle (CTR), E2 (10 nM), PPT (10 nM) or DPN (10 nM). The number of samples for each group was $n = 5$. (B) Relative levels of *Greb1* mRNA in WT, *Esr1*$^{-/-}$ or *Esr2*$^{-/-}$ AT29 cells treated for 24 h with either control vehicle (CTR) or E2 (10 nM). The number of samples for each group was $n = 3$. (C) Relative levels of *Greb1* mRNA in AT29 cells treated for 24 h with control vehicle (CTR) or E2 at 0.1, 1 or 10 nM. The number of samples for each group was $n = 4$. For each experiment, the relative abundance of mRNA was determined by RT-qPCR and normalized to mRNA levels of *B2m*. The horizontal bars and error bars represent the means ± SD, respectively. (D) Relative levels of *ESR1* (ERα) mRNA in GCTs ($n = 6$ patients) and granulosa cells (GCs) ($n = 12$ patients). (E) Relative levels of *GREB1* in granulosa cells (GCs) ($n = 12$ patients) and GCTs ($n = 6$ patients). The relative abundance of mRNAs was determined by RT-qPCR and normalized to mRNA levels of *GAPDH*. Each dot corresponds to one patient sample. (F) Relative amount of E2 (GCs, $n = 8$ patients; GCTs, $n = 6$ patients) determined by GC–MS and normalized by protein levels in each sample. Individual values are shown in a scatter plot with means as horizontal bars. (G) The relative levels of *GREB1* mRNA in (a) GCTs and (b) granulosa cells (GCs) were plotted against the relative content of E2 for each sample. Their possible correlations were analyzed by linear regression. Each dot represents one sample, with $n = 6$ (GCTs) and $n = 8$ (GCs) for E2 levels comparison. Data in A and B were analyzed with paired two-way ANOVA, and those in C with paired non-parametric one-way ANOVA (Friedman test). Data in D, E, and F were analyzed by a non-parametric *t*-test (Mann–Whitney). $^{*}p < 0.05$, $^{**}p < 0.01$, $^{***}p < 0.001$; NS, not significant.

control granulosa cells (Figure 5E). E2 content was 180-fold lower in GCTs than in granulosa cells (Figure 5F). Using correlation tests, we found that the relative expression level of *GREB1* in GCTs showed a significant positive correlation with E2 content ($R^2 = 0.7011$, $p = 0.0375$) (Figure 5Ga). Although not significant, there was a trend for a positive correlation in granulosa cells ($R^2 = 0.3258$, $p = 0.1395$) (Figure 5Gb). Altogether, these data support the idea that the abundance of *GREB1* could be dose-dependently regulated by E2 concentrations through ERα in GCTs.

Discussion

While retrospective studies on patients have reported that the response rate to AIs would be around 70%, a recent clinical trial that has enrolled about 40 patients suggests that it may be much lower [36]. The underlying mechanism behind such variability of the response to the hormonal therapy between patients is far from being understood, notably because of the lack of comprehensive analysis of E2 actions through its different receptors in this disease. Here, we provide, for the first time, experimental evidence that supports a direct role for E2 in promoting the growth of GCTs through ERs, with its action depending on the presence of the different subtypes of estrogen receptors.

Indeed, in agreement with previous reports, we observed that GPER, ERα, and ERβ can be expressed in primary and recurrent GCTs [7–9], but here we highlight their variable combination within our samples. In particular, we observed that in recurrent tumors ERα was no longer expressed alone, while ERβ was still expressed alone or at a high frequency in combination

with ERα compared with primary GCTs. In the present report, the percentages of GCTs expressing ERα or ERβ can differ from those in other studies [7,8,12,37]. These variable results could be due to the use of arbitrary cutoff points for interpreting positive immunoreactivity of TMA and to the use of different antibodies. However, a common feature between most studies including ours is that in recurrent GCTs, expression of ERβ is predominant over that of ERα. In addition, most primary and recurrent GCTs displayed GPER expression, including those without ERα and ERβ, indicating that E2 could have some effects through this receptor. Noteworthy, in primary and recurrent tumors that were considered as being ER-positive, only a subset of cells within the tumor expressed ERs and thus could be regulated by E2 through these receptors. All these observations led us to hypothesize that the response of primary and recurrent GCTs to E2 may vary according to at least two factors: (1) the type of receptor expressed and (2) the proportion of cells harboring estrogen receptivity.

Our cell-based studies using AT29 cells suggest that E2 could promote the growth and progression of GCTs by supporting cell survival, in agreement with a recent report showing that E2 enhances GCT cell viability in primary cultures [12]. Importantly, we found that this action of E2 in AT29 cells was reproduced by the treatment with two classically used selective ERα and ERβ agonists, but consistent with our previous observations in KGN cells [17], not with the GPER agonist. In AT29 cells, E2 growth-promoting action was lost in the absence of ERα but was not affected by the loss of ERβ. These results indicate that ERα is required in GCT cells for E2 to mediate its pro-survival action, whether ERβ is present or not. In contrast, when comparing our findings collected with the ERβ agonist (increasing GCT cell growth and survival) with those with the *Esr2* knockout clones (still reproducing full E2 action on GCT cell growth and survival), we infer that ERβ mediates GCT cell growth and survival only when ERα is present. Overall, these findings support the idea that AIs would have positive outcomes in patients with recurrent GCTs displaying ERα or combined ERα/ERβ expression, and probably not in those only expressing ERβ. However, additional studies are required to confirm this possibility, specifically in view of the fact that our findings were obtained from only one cell line. In addition, we cannot exclude the fact that ER-mediated action could be different when *FOXL2* is mutated on C402G, as this mutation may influence their reported interaction [38–40].

We also observed that the treatment with the GPER agonist G-1, but not with E2, led to decreased cell

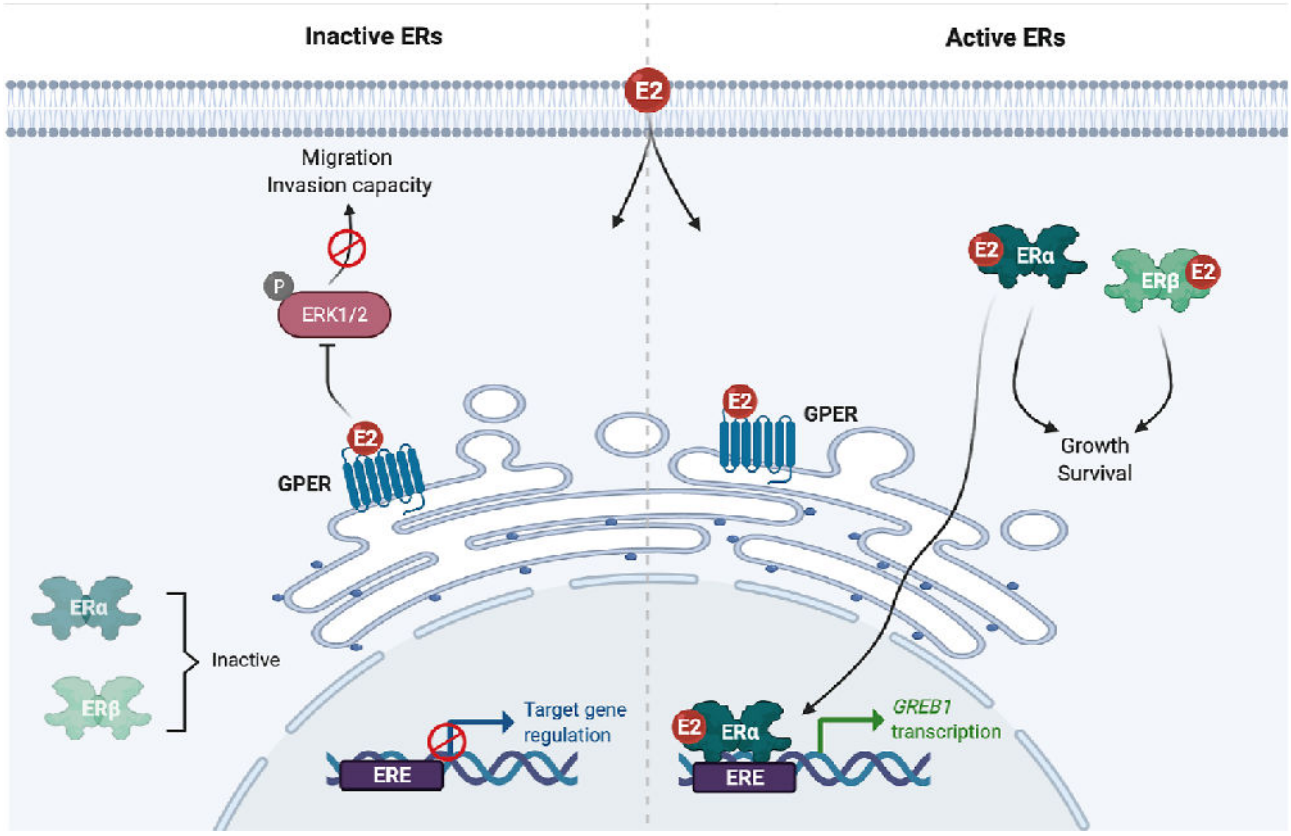

Figure 6. Proposed mechanisms of action of E2 in GCT cells. When ERs are present, estradiol (E2) would promote cell growth and survival through ERα-dependent genomic mechanisms, leading to *GREB1* upregulation upon binding to estrogen-response elements (EREs). E2 would also mediate its pro-tumor effect through an ERβ/ERα-dependent extra-nuclear mechanism that remains to be identified. In this context, GPER would not be activated by E2 to repress cell migration and invasion. In contrast, when ERs are inactive, GPER would be activated by E2 to repress ERK1/2 activity, thereby leading to decreased cell migration and invasion capacity [17].

migration and invasion capacity of AT29 cells. This is markedly different from what we obtained in the KGN tumoral granulosa cell line, wherein GPER signaling could be activated by both E2 and G-1 [17]. Since AT29 cells display active ERs, in contrast to KGN cells, it is tempting to speculate that E2 does not activate GPER signaling to inhibit cell spreading when cells express ERα and ERβ. Whether this could be due to the preferential binding of E2 to ERs over GPER (K_i of about 0.3 and 5.7 nM, respectively) needs to be investigated. If proven to be the case, E2 would either exert a growth-promoting effect in cells with active ERs or prevent metastatic spreading in GCTs expressing GPER and devoid of ER activity (Figure 6), but this hypothesis certainly deserves additional studies.

Our efforts to study ER mechanisms in GCT cells highlighted a possible distinct signaling pathway for ERα and ERβ. By using reporter assays, we demonstrated that ERα, but not ERβ, could act through an ERE-dependent mechanism in GCT cells, as reported in granulosa cells [41] (Figure 6). This finding was reinforced by the observation that the treatment with the ERα agonist PPT, but not that with the ERβ agonist DPN, upregulated the expression of *Greb1*, which would be required for E2-stimulated growth in a number of hormonally regulated tumors [42]. *Greb1* upregulation was lost in AT29 cells lacking ERα but not in those without ERβ, thus confirming the specificity of ERα activity on *Greb1* regulation in GCT cells. Our cell-based studies demonstrated that E2 exerted a concentration-dependent upregulation of this gene. Importantly, our subsequent analyses in human GCTs indicated that E2 concentrations may also influence the abundance of *GREB1 in vivo*, although we must be cautious with this interpretation due to limited sample size. From these observations, we hypothesize that the cancer-promoting action of E2 in GCTs could be related to the capacity of the tumor to synthesize this hormone. Since there was a trend for a significant correlation between *GREB1* expression and E2 content in granulosa cells, it is also tempting to speculate that aberrant exposure to high E2 levels, such as those occurring at the perimenopausal transition when GCTs frequently develop [43], could dramatically upregulate *GREB1* abundance to promote granulosa cell survival, thereby contributing to GCT initiation, but this issue warrants further studies.

The observed growth-promoting action of ERβ in GCTs contrasts with its tumor suppressor role observed in most cancers, such as breast and epithelial ovarian cancers, wherein ERβ opposes the pro-carcinogenic action of ERα [15]. On the other hand, ERβ has been proposed to promote cell survival and proliferation, not only in granulosa cells during folliculogenesis but also in non-small-cell lung cancers and endometriosis [44–46]. Therefore, it appears that ERβ has a pro- or an anti-tumor promoter role, depending on the cell context. Although the mechanism whereby it promotes GCT cell growth and survival remains unclear at present, one could assume that this receptor acts through an extra-nuclear mechanism, since we could observe ERβ expression in the cytoplasm in addition to the nucleus of human GCTs, as previously described [8]. This type of mechanism could involve plasma membrane ERβ rapidly relaying E2 action on signaling pathways such as those of MAPK ERK1/2 or PI3K [47], or mitochondrial ERβ regulating the release of cytochrome c from the mitochondria, thereby preventing cell apoptosis [48]. It would be of interest to determine in future studies whether this type of extra-nuclear mechanism could occur in GCTs and, in this case, how ERα contributes to ERβ activity, as suggested by our study.

In summary, this study presents strong evidence that E2 acts through its nuclear receptors to support GCT cell survival, thereby promoting primary and recurrent GCT growth and progression. This work highlights the high level of complexity of E2 action in GCTs driven by the different forms of estrogen receptors. It leads us to propose that ERα is required for mediating E2 action, and that ERβ, when expressed alone, may not be operative. These observations, together with the fact that only ∼40% of recurrent tumors express ERα, may explain the limited outcomes in patients under AI therapy. Future studies are needed to establish the possible link between the response of patients and the composition of the different ERs in their tumors.

Acknowledgements

We wish to thank Pr Nelly Frydman and Pr Michael Grynberg and their clinical staff at Antoine Béclère Hospital for their collaboration on granulosa cells, and Dr Sébastien Bouret (Institut du Cerveau et de la Möelle, Paris) for his critical review of the manuscript. We also acknowledge the valuable discussion on this work with Pr Reiner Veitia (Université de Paris, France). This work was supported by the Fondation Association pour la Recherche contre le Cancer, Gefluc Ile-de-France, the Institut National de la Santé et de la Recherche Médicale (Inserm), Center National de la Recherche Scientifique (CNRS), Université de Paris, and by doctoral fellowships from Ecole Doctorale Bio-SPC (VC, MMD).

Author contributions statement

VC, MMD, FP, FG, EA, DL, IT, SC, and CJG designed and performed the experiments and analyzed the data. AP, AM, AL, CG, SHK, and JK provided materials. VC, SC, and CJG prepared the figures and wrote the manuscript. VC, MMD, FG, JCT, SC, and CJG edited the manuscript.

Data availability statement

All data generated or analyzed during this study are included in this published article and its supplementary material files.

References

1. Schumer ST, Cannistra SA. Granulosa cell tumor of the ovary. *J Clin Oncol* 2003; **21:** 1180–1189.
2. Pectasides D, Pectasides E, Psyrri A. Granulosa cell tumor of the ovary. *Cancer Treat Rev* 2008; **34:** 1–12.
3. Miller K, McCluggage WG. Prognostic factors in ovarian adult granulosa cell tumour. *J Clin Pathol* 2008; **61:** 881–884.
4. Färkkilä A, Haltia UM, Tapper J, *et al*. Pathogenesis and treatment of adult-type granulosa cell tumor of the ovary. *Ann Med* 2017; **49:** 435–447.
5. Rey RA, Lhommé C, Marcillac I, *et al*. Antimüllerian hormone as a serum marker of granulosa cell tumors of the ovary: comparative study with serum alpha-inhibin and estradiol. *Am J Obstet Gynecol* 1996; **174:** 958–965.
6. Lappöhn RE, Burger HG, Bouma J, *et al*. Inhibin as a marker for granulosa-cell tumors. *N Engl J Med* 1989; **321:** 790–793.
7. Hutton SM, Webster LR, Nielsen S, *et al*. Immunohistochemical expression and prognostic significance of oestrogen receptor-alpha, oestrogen receptor-beta, and progesterone receptor in stage 1 adult-type granulosa cell tumour of the ovary. *Pathology* 2012; **44:** 611–616.
8. Ciucci A, Ferrandina G, Mascilini F, *et al*. Estrogen receptor β: potential target for therapy in adult granulosa cell tumors? *Gynecol Oncol* 2018; **150:** 158–165.
9. Chu S, Mamers P, Burger HG, *et al*. Estrogen receptor isoform gene expression in ovarian stromal and epithelial tumors. *J Clin Endocrinol Metab* 2000; **85:** 1200–1205.
10. Chu S, Nishi Y, Yanase T, *et al*. Transrepression of estrogen receptor beta signaling by nuclear factor-κB in ovarian granulosa cells. *Mol Endocrinol* 2004; **18:** 1919–1928.
11. Karnezis AN, Chen SY, Chow C, *et al*. Re-assigning the histologic identities of COV434 and TOV-112D ovarian cancer cell lines. *Gynecol Oncol* 2021; **160:** 568–578.
12. Haltia UM, Pihlajoki M, Andersson N, *et al*. Functional profiling of FSH and estradiol in ovarian granulosa cell tumors. *J Endocr Soc* 2020; **4:** bvaa034.
13. van Meurs HS, van der Velden J, Buist MR, *et al*. Evaluation of response to hormone therapy in patients with measurable adult granulosa cell tumors of the ovary. *Acta Obstet Gynecol Scand* 2015; **94:** 1269–1275.
14. Lamm W, Schiefer A, Nöbauer IM, *et al*. Aromatase inhibitor therapy as effective rescue in a patient with tamoxifen-refractory metastatic granulosa cell tumor of the ovary. *J Clin Oncol* 2016; **34:** e31–e33.
15. Jia M, Dahlman-Wright K, Gustafsson JÅ. Estrogen receptor alpha and beta in health and disease. *Best Pract Res Clin Endocrinol Metab* 2015; **29:** 557–568.
16. Hamilton KJ, Arao Y, Korach KS. Estrogen hormone physiology: reproductive findings from estrogen receptor mutant mice. *Reprod Biol* 2014; **14:** 3–8.
17. François CM, Wargnier R, Petit F, *et al*. 17β-estradiol inhibits spreading of metastatic cells from granulosa cell tumors through a non-genomic mechanism involving GPER1. *Carcinogenesis* 2015; **36:** 564–573.
18. Rae JM, Johnson MD, Scheys JO, *et al*. GREB1 is a critical regulator of hormone dependent breast cancer growth. *Breast Cancer Res Treat* 2005; **92:** 141–149.
19. Hodgkinson K, Forrest LA, Vuong N, *et al*. GREB1 is an estrogen receptor-regulated tumour promoter that is frequently expressed in ovarian cancer. *Oncogene* 2018; **37:** 5873–5886.
20. Ghosh MG, Thompson DA, Weigel RJ. *PDZK1* and *GREB1* are estrogen-regulated genes expressed in hormone-responsive breast cancer. *Cancer Res* 2000; **60:** 6367–6375.
21. Laviolette LA, Hodgkinson KM, Minhas N, *et al*. 17β-estradiol upregulates GREB1 and accelerates ovarian tumor progression *in vivo*. *Int J Cancer* 2014; **135:** 1072–1084.
22. Andersson S, Sundberg M, Pristovsek N, *et al*. Insufficient antibody validation challenges oestrogen receptor beta research. *Nat Commun* 2017; **8:** 15840.
23. Dutertre M, Gouédard L, Xavier F, *et al*. Ovarian granulosa cell tumors express a functional membrane receptor for anti-Müllerian hormone in transgenic mice. *Endocrinology* 2001; **142:** 4040–4046.
24. Nishi Y, Yanase T, Mu Y, *et al*. Establishment and characterization of a steroidogenic human granulosa-like tumor cell line, KGN, that expresses functional follicle-stimulating hormone receptor. *Endocrinology* 2001; **142:** 437–445.
25. Pierre A, Taieb J, Giton F, *et al*. Dysregulation of the anti-Müllerian hormone system by steroids in women with polycystic ovary syndrome. *J Clin Endocrinol Metab* 2017; **102:** 3970–3978.
26. Shah SP, Köbel M, Senz J, *et al*. Mutation of *FOXL2* in granulosa-cell tumors of the ovary. *N Engl J Med* 2009; **360:** 2719–2729.
27. Cluzet V, Devillers MM, Petit F, *et al*. Aberrant granulosa cell-fate related to inactivated p53/Rb signaling contributes to granulosa cell tumors and to FOXL2 downregulation in the mouse ovary. *Oncogene* 2020; **39:** 1875–1890.
28. Devillers MM, Petit F, Cluzet V, *et al*. FSH inhibits AMH to support ovarian estradiol synthesis in infantile mice. *J Endocrinol* 2019; **240:** 215–228.
29. Anttonen M, Färkkilä A, Tauriala H, *et al*. Anti-Müllerian hormone inhibits growth of AMH type II receptor-positive human ovarian granulosa cell tumor cells by activating apoptosis. *Lab Invest* 2011; **91:** 1605–1614.
30. Dong L, Wang H, Su Z, *et al*. Steroidogenic acute regulatory protein is a useful marker for Leydig cells and sex-cord stromal tumors. *Appl Immunohistochem Mol Morphol* 2011; **19:** 226–232.
31. Stauffer SR, Coletta CJ, Tedesco R, *et al*. Pyrazole ligands: structure–affinity/activity relationships and estrogen receptor-α-selective agonists. *J Med Chem* 2000; **43:** 4934–4947.
32. Meyers MJ, Sun J, Carlson KE, *et al*. Estrogen receptor-β potency-selective ligands: structure–activity relationship studies of diarylpropionitriles and their acetylene and polar analogues. *J Med Chem* 2001; **44:** 4230–4251.
33. Bologa CG, Revankar CM, Young SM, *et al*. Virtual and biomolecular screening converge on a selective agonist for GPR30. *Nat Chem Biol* 2006; **2:** 207–212.
34. Paech K, Webb P, Kuiper GG, *et al*. Differential ligand activation of estrogen receptors ERα and ERβ at AP1 sites. *Science* 1997; **277:** 1508–1510.
35. Inaoka Y, Yazawa T, Uesaka M, *et al*. Regulation of NGFI-B/Nur77 gene expression in the rat ovary and in Leydig tumor cells MA-10. *Mol Reprod Dev* 2008; **75:** 931–939.
36. Banerjee SN, Tang M, O'Connell R, *et al*. PARAGON: a phase 2 study of anastrozole (An) in patients with estrogen receptor (ER) and / progesterone receptor (PR) positive recurrent/metastatic granulosa cell tumors/sex-cord stromal tumors (GCT) of the ovary. *J Clin Oncol* 2018; **36:** 5524–5524.
37. Farinola MA, Gown AM, Judson K, *et al*. Estrogen receptor α and progesterone receptor expression in ovarian adult granulosa cell tumors and Sertoli-Leydig cell tumors. *Int J Gynecol Pathol* 2007; **26:** 375–382.
38. Kim SY, Weiss J, Tong M, *et al*. Foxl2, a forkhead transcription factor, modulates nonclassical activity of the estrogen receptor-α. *Endocrinology* 2009; **150:** 5085–5093.
39. Fleming NI, Knower KC, Lazarus KA, *et al*. Aromatase is a direct target of FOXL2: C134W in granulosa cell tumors via a single highly conserved binding site in the ovarian specific promoter. *PLoS One* 2010; **5:** e14389.
40. Georges A, L'Hôte D, Todeschini AL, *et al*. The transcription factor FOXL2 mobilizes estrogen signaling to maintain the identity of ovarian granulosa cells. *Elife* 2014; **3:** e04207.
41. Mueller SO, Katzenellenbogen JA, Korach KS. Endogenous estrogen receptor β is transcriptionally active in primary ovarian

cells from estrogen receptor knockout mice. *Steroids* 2004; **69:** 681–686.
42. Cheng M, Michalski S, Kommagani R. Role for growth regulation by estrogen in breast cancer 1 (GREB1) in hormone-dependent cancers. *Int J Mol Sci* 2018; **19:** 2543.
43. Hale GE, Burger HG. Hormonal changes and biomarkers in late reproductive age, menopausal transition and menopause. *Best Pract Res Clin Obstet Gynaecol* 2009; **23:** 7–23.
44. Drummond AE, Fuller PJ. The importance of ERbeta signalling in the ovary. *J Endocrinol* 2010; **205:** 15–23.
45. Miki Y, Abe K, Suzuki S, *et al*. Suppression of estrogen actions in human lung cancer. *Mol Cell Endocrinol* 2011; **340:** 168–174.
46. Chantalat E, Valera MC, Vaysse C, *et al*. Estrogen receptors and endometriosis. *Int J Mol Sci* 2020; **21:** 2815.
47. Levin ER. Integration of the extranuclear and nuclear actions of estrogen. *Mol Endocrinol* 2005; **19:** 1951–1959.
48. Pedram A, Razandi M, Wallace DC, *et al*. Functional estrogen receptors in the mitochondria of breast cancer cells. *Mol Biol Cell* 2006; **17:** 2125–2137.

SUPPLEMENTARY MATERIAL ONLINE

Figure S1. Validation of the primary antibody against ERβ

Figure S2. Validation of *Esr1*$^{-/-}$ and *Esr2*$^{-/-}$ AT29 cell clones

Figure S3. GPER, ERα, and ERβ expression in primary and recurrent GCTs

Figure S4. Characterization of AT29 and KGN cells

Figure S5. BrdU incorporation assays

Figure S6. Validation of the AP-1-luciferase reporter system in MCF-7 cells

Figure S7. *ESR2* mRNA levels in GCs and GCTs

Table S1. Clinical information of the patients enrolled in the TMA study

Table S2. Primers used for qPCR